AIP | Applied Physics Letters

Resonant carrier scattering by core-shell nanoparticles for thermoelectric power factor enhancement

Je-Hyeong Bahk, Parthiban Santhanam, Zhixi Bian, Rajeev Ram, and Ali Shakouri

Citation: Applied Physics Letters **100**, 012102 (2012); doi: 10.1063/1.3673615
View online: http://dx.doi.org/10.1063/1.3673615
View Table of Contents: http://scitation.aip.org/content/aip/journal/apl/100/1?ver=pdfcov
Published by the AIP Publishing

Resonant carrier scattering by core-shell nanoparticles for thermoelectric power factor enhancement

Je-Hyeong Bahk,[1,a),b)] Parthiban Santhanam,[2,a),b)] Zhixi Bian,[1] Rajeev Ram,[2] and Ali Shakouri[1]
[1]*Department of Electrical Engineering, University of California, Santa Cruz, California 95064, USA*
[2]*Department of Electrical Engineering and Computer Science, Massachusetts Institute of Technology, Cambridge, Massachusetts 02139, USA*

(Received 2 November 2011; accepted 9 December 2011; published online 3 January 2012)

We theoretically investigate the use of energetically sharp resonances of core-shell nanoparticles embedded in semiconductors to selectively scatter carriers and thereby enhance the thermoelectric power factor and figure of merit. Appropriate selection of materials for the core-shell band structure can lead to the formation of quasi-bound states inside the nanoparticles, which strongly scatter carriers near these energy levels, making sharp features in the energy-dependent electron relaxation time. We find that the power factor of PbTe at 80 K is enhanced by more than 80% when core-shell nanoparticles of 3 nm core diameter and 1.5 nm shell width are introduced with density 1×10^{18} cm^{-3}. © *2012 American Institute of Physics*. [doi:10.1063/1.3673615]

The efficiency of thermoelectric devices directly depends on the dimensionless figure of merit, $ZT = S^2\sigma T/\kappa$, of the materials used, where S is the Seebeck coefficient, σ is the electrical conductivity, T is the absolute temperature, and κ is the thermal conductivity, respectively. In recent years, significant enhancements in the thermoelectric figure of merit have been achieved mainly by reducing the thermal conductivity via the introduction of additional phonon scattering in nanostructured materials such as superlattices and nanocomposites.[1–4]

However, only a few methods have been reported for enhancing the so-called power factor, $S^2\sigma$, in the numerator of ZT. Hicks and Dresselhaus theoretically predicted improved power factor by the modified density of states in low-dimensional materials such as quantum wells and wires in 1993.[5] Since then, a great deal of research activities has been carried out on various nanostructured materials for thermoelectric energy conversion.[6,7] The ErAs nanoparticles embedded in InGaAlAs III-V semiconductors showed both thermal conductivity reduction and power factor enhancement to reach $ZT \sim 1.3$ at 800 K.[4] However, the magnitude of the power factor enhancement has not been fully explained as the details of the scattering potential and band profile around nanoparticles are not yet known. Recently, the modulation doping concept has been experimentally demonstrated in SiGe nanocomposites to improve electrical conductivity over bulk values, thus enhancing the power factor.[8] Bahk *et al.* also proposed that the electrical conductivity and power factor can be enhanced when embedded nanoparticles of a few nm in diameter donate charge carriers instead of the conventional impurity dopants.[9]

Recently, Heremans *et al.* demonstrated a large power factor enhancement in Tl-doped PbTe at high temperatures, and attributed this enhancement to the distorted density of states (DOS) by the Tl resonant level inside the valence band of PbTe.[10] Group III elements such as Tl, and group IV elements such as Sn have also been found to create resonant levels in the band structures of IV-VI semiconductors,[11] and Bi_2Te_3,[12] respectively. The effect of resonant impurity levels on thermoelectric transport comes in two distinct ways: the modified density of states[10,11] and the resonant carrier scattering,[12,13] both of which, however, result in similar Seebeck coefficient enhancements by increasing the slope of differential conductivity with respect to energy. The resonant carrier scattering improves the thermoelectric properties mainly at low temperatures.

In this letter, we propose the use of core-shell nanoparticles embedded in bulk semiconductors as resonant scattering centers to suppress conduction in a narrow band of energies and thereby enhance the Seebeck coefficient and thermoelectric power factor. Fig. 1 shows the three-dimensional structure of the proposed core-shell nanoparticles and the potential profile around them in the radial direction, r. The core region ($r < a$) forms a potential well with the well depth V_0 below the band minimum of the host material, and the shell region ($a < r < b$) forms a potential barrier around the core with the finite barrier height V_1 above the host band minimum. When an appropriate potential

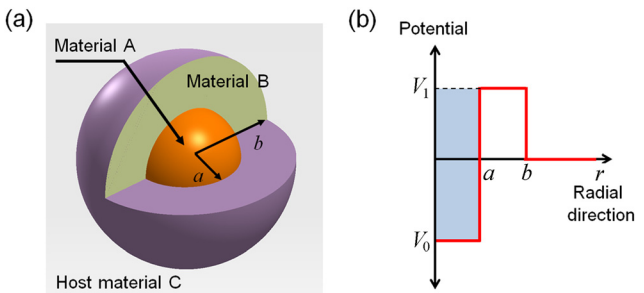

FIG. 1. (Color online) (a) Three dimensional schematic of the proposed core-shell nanoparticle structure and (b) potential profile around the nanoparticles in radial direction. The core region ($r < a$) has heavier effective mass (i.e., 1 to 1.2m_0) than those of the shell region and the host material (i.e., 0.053m_0, the density of states effective mass of PbTe at 80 K).

[a)]J.-H. Bahk and P. Santhanam contributed equally to this work.
[b)]Authors to whom correspondence should be addressed. Electronic addresses: jhbahk@soe.ucsc.edu and parthi@mit.edu.

profile is used along with the proper selection of materials for the effective masses of the core and shell regions, quasi-bound states are formed inside the core with evanescent tails that resonantly couple to the continuum of free electron states in the host conduction band.

Fig. 2 shows the energy-dependent scattering times of the core-shell nanoparticles for varying well depth (V_0) calculated using the partial wave method.[14] In dilute regime of particles as in this work, scattering events are independent, and thus the total scattering time is inversely proportional to the particle density. When the particle density is so high that the scattering events are no longer independent, the coherent potential approximation method can be used for the scattering calculations.[15] All the parameters for the core-shell nanoparticles are carefully chosen to have one quasi-bound state between the matrix conduction band minimum and the barrier height. We used $1.2m_0$ for the core effective mass, and $0.053m_0$ for the shell and host material. The size of the core radius a is chosen to be 1.5 nm, and the shell width (b-a) to be 1.5 nm as well. The barrier height V_1 is 0.2 eV, and the well bottom V_0 is varied to control the position of the quasi-bound state. For the core material, metals that have large effective masses around 1 to $1.2m_0$ can be used. The shell material can be an alloy of the host material with small stoichiometric difference so that the band offset is limited to 0.2 or 0.3 eV, and the effective mass remains similar to the host mass.

In Fig. 2, strong scattering dips are observed at the quasi-bound energy levels, which shift to higher energy as V_0 goes up. These sharp scattering dips are clear evidence of the strong resonance between free electrons and the quasi-bound state inside the core-shell nanoparticle. Near the resonance, the energy-dependence of the scattering rate is approximately Lorentzian.[13] The width of the resonant dip comes from the homogeneous broadening of the resonant level due to the finite lifetime of electron in the quasi-bound state. Electrons remain in the localized quasi-bound state for a certain amount of time, i.e., the state's lifetime, and are ejected out of the state with a randomized momentum. As the electron is confined in the state more weakly (i.e., by thinner and lower barriers, shallower well depth, and/or smaller core size), this lifetime decreases. By the energy-time uncertainty principle, the shorter lifetime in the state results in larger uncertainty of the energy level, and the resonance becomes wider.

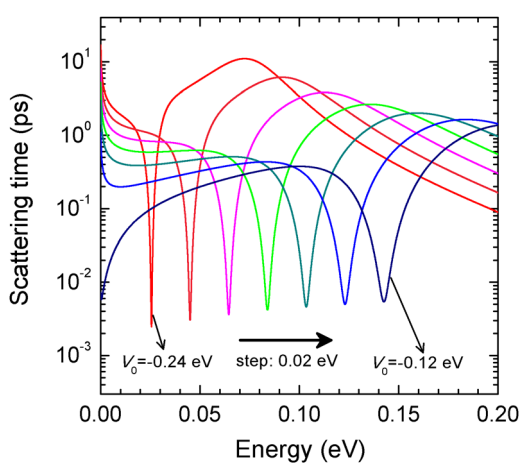

FIG. 2. (Color online) Scattering time of 1×10^{18} cm^{-3} core-shell nanoparticles as a function of electron energy for varying well bottom in the core from $V_0 = -0.24$ eV to -0.12 eV with a step size of 0.02 eV. Other parameters of the core-shell nanoparticles are all assumed to be constants as $V_1 = 0.2$ eV, $a = 1.5$ nm, $b = 3$ nm, $m^*_{in} = 1.2m_0$, and $m^*_{out} = 0.053m_0$.

The scattering time at energies far away from the resonant levels is determined predominantly by non-resonant scatterings of electrons, such as interface scattering at the potential boundaries. The presence of this additional non-resonant scattering is an important difference between core-shell nanoparticles and impurities that similarly lead to resonant scattering. The sharp potential boundary is associated with the scattering of high energy electrons through the Fourier transform.[9] Moreover, since the range of the nanoparticle sizes of interest falls in the Rayleigh scattering regime, the scattering time monotonically decreases with increasing energy for the non-resonant scattering as shown at the energies far away from the resonant dips in Fig. 2. Note that another bound state with energy just below the host band edge may dominate over non-resonant scattering at low energies as when $V_0 = -0.12$ eV in Fig. 2. The non-resonant scattering rates vary slowly with energy, and diminish the slope of the energy-dependent scattering time at the shoulders of the resonance dips, thereby reducing their enhancement of the Seebeck coefficient. As a result, it is necessary to keep the non-resonant scattering weak with the barrier height sufficiently low (<0.3 eV in most cases) and the size of core-shell nanoparticles sufficiently small (a few nm) in order to gain a large Seebeck enhancement by resonant scattering.

The comparison of the differential scattering cross sections as a function of electron momentum in Fig. 3 reveals clear distinction between the resonant scattering and the Rayleigh-like non-resonant scattering. In Fig. 3(a), the same effective mass of $0.053m_0$ is used everywhere in both core and shell region, so that there is no resonant level formed. On the other hand, a large effective mass of $1.2m_0$ is used for the core in Fig. 3(b), so that there is a resonant state

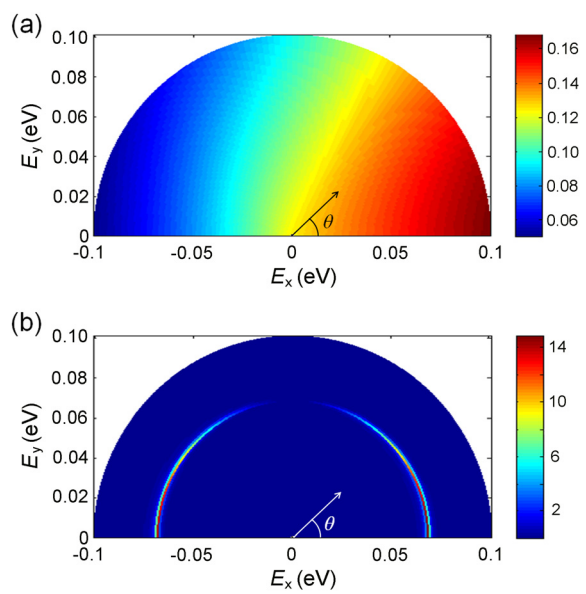

FIG. 3. (Color online) Differential scattering cross section in units of πa^2 (cross section of core region) as a function of final electron momentum (polar angle and magnitude) for core-shell nanoparticles with (a) non-resonant scattering and (b) resonant scattering with resonant energy level at ~0.07 eV. The incident wave propagates to the +x-direction from left to right.

formed at ~0.07 eV. The non-resonant scattering has slowly varying differential scattering cross-section with energy and angle. Electrons of greater energy are scattered more, and scattering is primarily by small angles. On the other hand, the resonant scattering is very strong only near the resonant level, and the electron is scattered both forward and backward with almost equal probability, since the resonant state is sharply localized in real space.

Fig. 4 shows the thermoelectric transport properties of PbTe embedded with the core-shell nanoparticles of $1 \times 10^{18}\,\mathrm{cm}^{-3}$ density at 80 K, calculated based on the Boltzmann transport theory under the relaxation time approximation.[16] The core-shell nanoparticle scattering as well as other major scattering mechanisms in PbTe such as polar optical phonon scattering, non-polar optical phonon and acoustic phonon deformation potential scatterings, alloy scattering, and the screened Coulomb impurity scattering are all included in the calculations using the band and scattering parameters given by the previous literature.[17,18] We have included the strong dielectric screening effect in the phonon scattering calculations for the IV-VI semiconductor.[19] A non-parabolic band model is used for the bulk PbTe. PbTe is selected as the host material, because it has large power factors over a wide temperature range, and compared to phonon scattering, the ionized impurity scattering rate in this material is negligibly small even at very high carrier density, so that its mobility is relatively unchanged even with strong doping. These characteristics allow us to probe the effects of core-shell nanoparticle scattering over a wide range of doping densities without making more idealized assumptions about additional electron scattering processes.

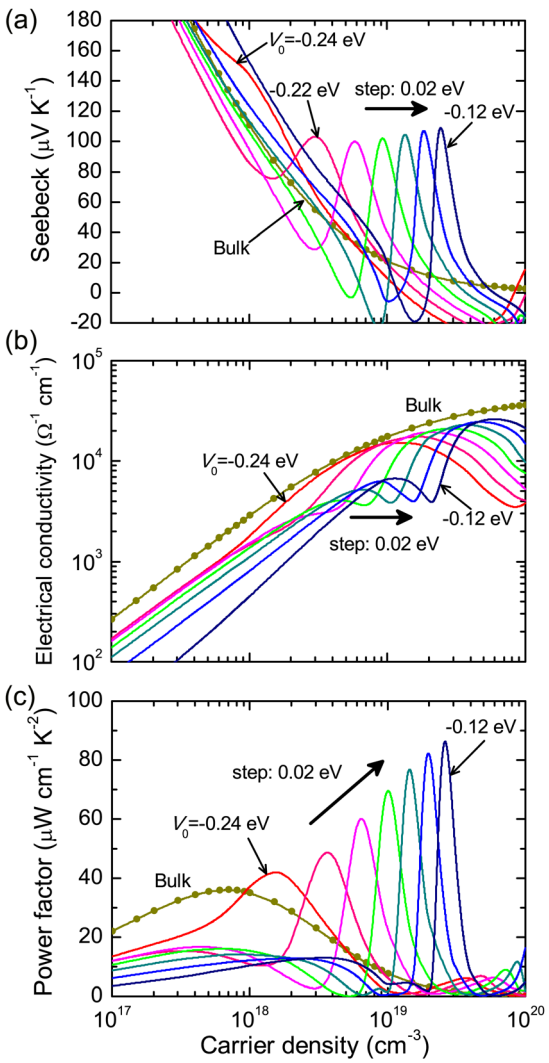

FIG. 4. (Color online) (a) Seebeck coefficient, (b) electrical conductivity, and (c) power factor of PbTe with $1 \times 10^{18}\,\mathrm{cm}^{-3}$ core-shell nanoparticles embedded in comparison with bulk PbTe values as a function of carrier density at 80 K. The parameters of the core-shell nanoparticles used in these plots are the same as those used in Fig. 2 with varying well bottom (V_0).

As can be seen in Fig. 4(a), the Seebeck coefficient sharply increases in a narrow carrier density range for the core-shell nanoparticle materials indicating more than a 10-fold enhancement over the bulk value with the equivalent carrier density. As the carrier density is changed from low to high, the Fermi level increases in energy accordingly; when the Fermi level passes by the energy window in which the resonant scattering time has a sharp positive slope, i.e., at the high energy end of the resonant dip, the Seebeck coefficient is drastically enhanced. This is due to the highly selective carrier scattering which allows higher energy electrons to conduct better than lower energy ones, so that the average electron energy and thus the Seebeck coefficient are increased. This effect is less significant at higher temperatures because the energy distribution of electrons participating in electrical conduction is broader at higher temperatures, proportional to $k_B T$, according to the Fermi-Dirac distribution, so that a larger portion of electrons may not see the much sharper resonance and not benefit from the selective resonant carrier scattering at higher temperatures. In fact, the peak of the Seebeck coefficient in Fig. 4(a) slightly increases with V_0, indicating that further broadening could actually improve the material's power factor. As V_0 increases, the resonant level shifts up and broadens at the same time, so the maximum Seebeck coefficient may keep increasing with increasing V_0 until the broadening of the resonance exceeds the optimal width. Fig. 4(a) also shows that resonant scattering may even reverse the sign of the Seebeck coefficient. When the Fermi level falls along the lower-energy side of the resonance and the slope of the scattering time with energy is sharply negative, the states above the Fermi level see lower mobility than those below it. As a result, in spite of the greater density of states above the Fermi level, the average transport energy is below the Fermi level and the sign of the Seebeck coefficient is reversed.

The mobility and the electrical conductivity are suppressed at the resonances due to the strong scattering as shown in Fig. 4(b). However, when the Fermi level is aligned properly at the high-energy shoulder of the resonance, the scattering time retains a large slope which enhances the Seebeck coefficient, but the scattering time remains sufficiently high across the Fermi window to keep overall mobility high as well. This alignment maximizes the power factor as a function of doping. As shown in Fig. 4(c), the power factor is enhanced to 65 μW/cmK^2 or higher when the well bottom V_0 is higher than −0.2 eV, which is a more than 80% enhancement over the maximum bulk power factor 36 μW/cmK^2. The maximum power factor will keep increasing with increasing V_0 until the broadening of the resonance starts to decrease the Seebeck enhancement, or the suppression of mobility at the optimal carrier density outweighs the diminishing Seebeck enhancement.

In summary, core-shell nanoparticles having resonant levels within the band of the host material can significantly enhance the thermoelectric power factor over the bulk at low temperatures. This is due to the large Seebeck enhancement by the sharp features in the modified scattering time. More than 80% of power factor enhancement could be obtained in PbTe at 80 K. At high temperatures, these enhancements would be smaller due to the wide electron energy distribution and the stronger phonon scattering. A systematic study on the effect of the various conditions of the core-shell resonant scattering at high temperatures is a subject of future publication.

The authors are grateful to Mona Zebarjadi for her great contribution to the partial wave code. This work was partly supported by DARPA/NMP.

[1]R. Venkatasubramanian, E. Siivola, T. Colpitts, and B. O'Quinn, Nature **413**, 597 (2001).
[2]K. F. Hsu, S. Loo, F. Guo, W. Chen, J. S. Dyck, C. Uher, T. Hogan, E. K. Polychroniadis, and M. G. Kanatzidis, Science **303**, 818 (2004).
[3]B. Poudel, Q. Hao, Y. Ma, Y. C. Lan, A. Minnich, B. Yu, X. Yan, D. Z. Wang, A. Muto, D. Vashaee *et al.*, Science **320**, 634 (2008).
[4]J. M. O. Zide, J.-H. Bahk, R. Singh, M. Zebarjadi, G. Zeng, H. Lu, J. P. Feser, D. Xu, S. L. Singer, Z. X. Bian *et al.*, J. Appl. Phys. **108**, 123702 (2010). Erratum: J. Appl. Phys. **110**, 059902 (2011).
[5]L. D. Hicks and M. S. Dresselhaus, Phys. Rev. B **47**, 12727 (1993).
[6]C. J. Vineis, A. Shakouri, A. Majumdar, and M. G. Kanatzidis, Adv. Mater. **22**, 3970 (2010).
[7]A. Shakouri, Annu. Rev. Mater. Res. **41**, 399 (2011).
[8]M. Zebarjadi, G. Joshi, G. Zhu, B. Yu, A. Minnich, Y. Lan, X. Wang, M. Dresselhaus, Z. Ren, and G. Chen, Nano Lett. **11**, 2225 (2011).
[9]J.-H. Bahk, Z. Bian, M. Zebarjadi, P. Santhanam, R. Ram, and A. Shakouri, Appl. Phys. Lett. **99**, 072118 (2011).
[10]J. P. Heremans, V. Jovovic, E. S. Toberer, A. Saramat, K. Kurosaki, K. Charoenphakdee, S. Yamanaka, and J. F. Snyder, Science **321**, 554 (2008).
[11]S. Ahmad, K. Hoang, and S. D. Mahanti, Phys. Rev. Lett. **96**, 056403 (2006).
[12]M. K. Zhitinskaya, S. A. Nemov, and T. E. Svechnikova, Phys. Solid State **40**, 1297 (1998).
[13]Y. I. Ravich, in *CRC Handbook of Thermoelectrics*, edited by D. M. Rowe (CRC, Boca Raton, FL, 1995), Chap. 7, p. 67.
[14]M. Zebarjadi, K. Esfarjani, A. Shakouri, J.-H. Bahk, Z. Bian, G. Zeng, J. E. Bowers, H. Lu, J. M. O. Zide, and A. C. Gossard, Appl. Phys. Lett. **94**, 202105 (2009).
[15]M. Zebarjadi, K. Esfarjani, Z. Bian, and A. Shakouri, Nano Lett. **11**, 225 (2011).
[16]J.-H. Bahk, Z. Bian, M. Zebarjadi, J. M. O. Zide, H. Lu, D. Xu, J. P. Feser, G. Zeng, A. Majumdar, A. C. Gossard *et al.*, Phys. Rev. B **81**, 235209 (2010).
[17]C. J. Vineis, T. C. Harman, S. D. Calawa, M. P. Walsh, R. E. Reeder, R. Singh, and A. Shakouri, Phys. Rev. B **77**, 235202 (2008).
[18]D. I. Bilc, S. D. Mahanti, and M. G. Kanatzidis, Phys. Rev. B **74**, 125202 (2006).
[19]Y. I. Ravich, B. A. Efimova, and V. I. Tamarchenko, Phys. Status Solidi B **43**, 11 (1971).